STUDIA UBB CHEMIA, LIX, 4, 2014 (p. 103-112)
(RECOMMENDED CITATION)

THEORETICAL STUDY ON NITROGEN TRIFLUORIDE AND ITS ADDUCT WITH BF_3

HONGCHEN DU[a,*], PING YANG[a], LIJUN ZHANG[a], YU WANG[b,*]

ABSTRACT. The molecular and crystal structure of the adduct $NF_3 \cdot BF_3$ has been studied using complete basis set method (CBS-4M). It shows that the adduct exists in the form of complex but not ionic, the heat of formation of the gas and condensed phase of the adduct are -1266.09 and -1276.37 kJ·mol-1 respectively, which denotes it is stable under atmospheric conditions. The crystal form tends to crystalline in P21/c space group. The large calculated band gap (ΔEg) of the crystal proves it is stable, which is consistent with the conclusion from gas phase. The conduction band (LUCO) is mainly contributed from the *p* state of N atom and valence band (HOCO) from the *p* state of F atom.

Keywords: *molecular, crystal, structure, property, theoretical study*

INTRODUCTION

Molecular complexes containing boron trifluoride as a Lewis acid have been known for many years [1]. Nitrogen trifluoride (NF3) is a colorless, toxic, odourless, nonflammable gas, it was first prepared in 1928 by Ruff, Fischer, and Luft [2] by electrolyzing molten anhydrous ammonium bifluoride in an electrically heated copper cell. Nitrogen trifluoride can also be formed by the direct fluorination of ammonia. It is a stable gas with strong oxidizing properties, can be used as a potential oxidant for space-craft propulsion. Decades ago, the studies on the compound had been performed: the infrared spectrum of NF_3 has been reported by Bailey, Hale, and Thompson [3]. In 1950, NF_3 had been shown to have the C_{3v} symmetry [4,5].

Today nitrogen trifluoride is predominantly employed in the cleaning of the PECVD chambers in the high volume production of liquid crystal displays and silicon-based thin film solar cells. NF3 has been considered as an environmentally preferable substitute for sulfur hexafluoride or perfluorocarbons

[a] *School of Science, Zhejiang A & F university, Linan, 311300, China*
[b] *Zhejiang Provincial Key Laboratory of Chemical Utilization of Forestry Biomass, Zhejiang A & F University, Linan, 311300, China*
** Corresponding authors: duhongc@zafu.edu.cn, yuwang79@gmail.com*

such as hexafluoroethane [6]. It proved to be far less reactive than the other nitrogen trihalides such as nitrogen trichloride, nitrogen tribromide and nitrogen triiodide, all of which are explosive. But explosion will occur when mixtures of nitrogen trifluoride with ammonia, hydrogen, methane, ethylene, carbon monoxide.

Understanding the nature of the structure-property relationship is of the fundamental importance for further investigation. However, the investigation on structure property relationship especially the crystal structure of NF_3 with BF_3 are limited, in 1996, Ford et al. performed a theoretical study on the adduct using *ab initio* method mainly about its binding energies [7].

As the adduct has similar properties with high energy density materials (HEDMs) which we are interested in, i.e., it is reactive and highly energetic but still stable enough under certain conditions, but the available information about it is limited, so we performed this study to predict its molecular and crystal structures and corresponding properties with the complete basis set method.

COMPUTATIONAL METHODS

The title compound was optimized at CBS-4M level, and vibrational analysis was performed thereafter for the most stable conformer with the Gaussian 03 program package [8].

The gas phase heat of formation ($\Delta_f H°_{gas}$) was obtained using the following reaction:

$$NF_3+BF_3=NF_3\cdot BF_3$$

The changes in enthalpy (ΔH°_{298}) of the above reactions were evaluated using the following equation:

$$\Delta H^{\circ}_{298} = \sum \Delta_f H^{\circ}_{298,\mathrm{P}} - \sum \Delta_f H^{\circ}_{298,\mathrm{R}} = \Delta E_0 + \Delta E_{\mathrm{ZPE}} + \Delta H^{\circ}_{T} + \Delta \mathrm{nRT}$$

where $\sum \Delta_f H^{\circ}_{298,\mathrm{P}}$ and $\sum \Delta_f H^{\circ}_{298,\mathrm{R}}$ are the sum of the heats of formation of the products and reactants, respectively; ΔE_0 is the difference between the total energies of the products and the reactants at 0 K; ΔE_{ZPE} is the difference between the zero-point vibrational energy of the products and the reactants; ΔH^{0}_{T} is the difference between the thermal correction from 0 K to 298 K of the products and the reactants, Δn is the change in the quantity of gaseous substances, which is -1 here. In the reactions above, the experimental heats of formation of all reactants (BF_3, NF_3) are known [9], the heats of formation of the adduct can then be obtained with the calculated ΔH°_{298}.

Interaction energies were estimated from the energy differences between NF3 and BF3. The basis sets commonly used to calculate energies are far from being saturated. As a result, each sub-system in any complex will tend to lower its energy depending on the use of basis set functions of the other sub-system. The energies obtained at equilibrium geometry of complex for each sub-system are lower than those calculated at the same geometry with basis set functions of respective sub-system alone. This energy difference is so-called basis set superposition error (BSSE). The binding energies of the supermolecules are equal to the differences between the supermolecules and the monomers after correcting for the BSSE energies.

On the basis of the principle of statistical thermodynamics [10], standard molar heat capacity ($C^0_{p,m}$), entropy (S^0_m), and enthalpy (H^0_m) from 200 to 800 K were evaluated using the scaled frequencies.

To find the possible molecular packings in crystal phase, empirical Dreiding force field and polymorph module in MS [11] were used. Since most crystals belong to 7 space groups (P21/c, P-1, P212121, P21, Pbca, *C2/c*, and Pna21) on the basis of statistical data [12-15], the global search was confined in these groups only. By analyzing the simulation trajectory of molecular packing within 7 space groups, the structures were arranged in their ascending energies for each group and the one having the lowest energy was selected as the most possible packing with the corresponding space group. These possible crystal structures were then refined with the DFT GGA-RPBE method and CASTEP module [16].

RESULTS AND DISCUSSION

Molecular Structure

Figure 1 (left) lists the molecular structure of adduct under CBS-4M level, it can be seen that in unit of NF_3, the bond length of N-F are all similar but N1-F3 is slightly larger, which denotes N1-F3 is weaker. The bond length of B5-F3 is 2.33 Å, thus the bond is very weak. In addition, the negative charges on F(3) (-0.195e) is also similar with F(2) and F(4), implying the same properties between F(3) and other F atoms. The total charges of NF3 and BF_3 are nearly zero (0.075e and -0.075e), therefore, adduct exists in basically the complex form $NF_3 \cdot BF_3$ but not ionic form.

Sorescu et al. performed theoretical predictions for several energetic molecular crystals, and claimed that the dispersion-corrected density functional theory (DFT-D) method as parametrized by Grimme provides significant improvements for the description of intermolecular interactions in molecular crystals at both ambient and high pressures relative to conventional DFT [17]. Thus, DFT-D calculations are also included. DFT-D method was used in this article, Binding energy of the complex is only about -10 $kJ \cdot mol^{-1}$.

Figure 1 (right) lists the molecular structure of the adduct under DFT-D level, we can see that the molecular structures are similar with each other.

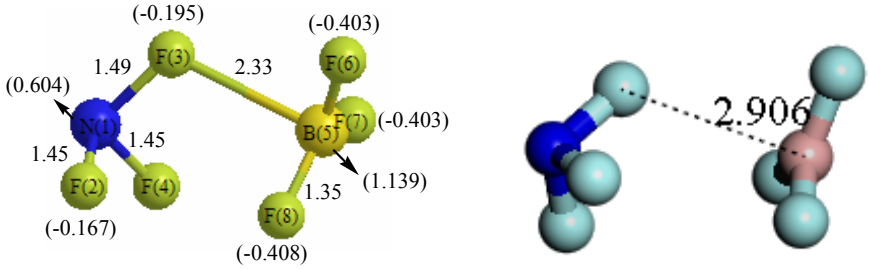

Figure 1. Structural parameters of the adduct obtained at CBS-4M (left) and DFT-D levels (bond lengths are in Å, Mulliken charges (in brackets) in e)

The molecular electrostatic potential (MEP) is used commonly in analyzing molecular reactivity and is very useful since it provides information about local polarity due to the charge density distribution. After having chosen some sort of region to be visualized, a color-coding convention is chosen to depict the MEP. Figure 2 illustrates the MEP for the 0.001 electron/bohr^3 isosurface of electron density at the CBS-4M level for the $NF_3 \cdot BF_3$, The color with red denoting the most negative potential and blue denoting the most positive potential. Inspection of the MEP for the title compound, the negative potentials appear to be distributed mostly on the fluoride atoms, and the positive ranges characterize at the center of the skeleton mainly on the nitrogen and boron atom. After taking into account of the basis set superposition error (BSSE), we found that the binding energy of the complex is only about -10 kJ·mol^{-1}.

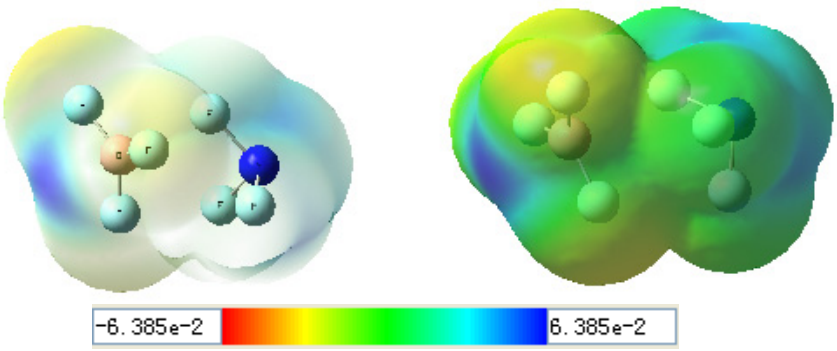

Figure 2. Molecular electrostatic potential (MEP) surface mapped onto 0.001 electron/bohr^3 controur of the electronic density for the title compound calculated at the CBS-4M level

Thermodynamic Properties

Based on the scaled vibrational frequencies and the principle of statistic thermodynamics, the standard thermodynamic properties are evaluated and shown in Figure 3. Obviously, with the increasing temperature, all the thermodynamic properties increase, which is mainly because the vibrational movement is intensified at the higher temperature and therefore makes more contributions to the thermodynamic properties. The relationships between the thermodynamic functions and temperature are found and shown as follows (the units of $C^{\circ}_{p,m}$, S°_{m}, H°_{m} are $J \cdot K^{-1} \cdot mol^{-1}$, $J \cdot K^{-1} \cdot mol^{-1}$, $kJ \cdot mol^{-1}$, respectively, and the correlation coefficients are 0.9940, 0.9996, and 0.9999 respectively):

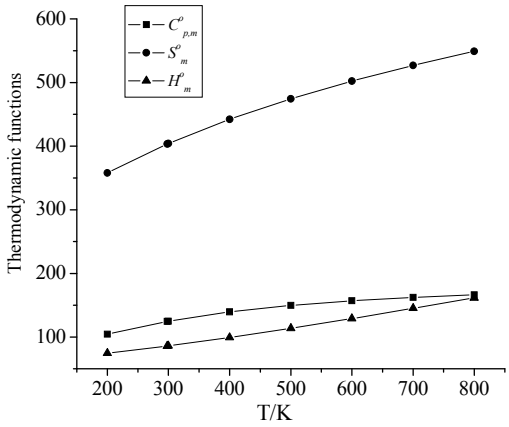

Figure 3. Relationships between the thermodynamic functions and temperature

$$C^{\circ}_{p,m} = 60.29 + 0.25\,T - (1.60\times10^{-4})T^2$$

$$S^{\circ}_{m} = 259.62 + 0.54\,T - (2.35\times10^{-4})T^2$$

$$H^{\circ}_{m} = 52.49 + 0.09\,T + (4.77\times10^{-5})T^2$$

From these equations, we have

$$\frac{dC^{o}_{p,m}}{dT} = 0.25 - (3.20\times10^{-4})T$$

$$\frac{dS^{o}_{m}}{dT} = 0.54 - (4.70\times10^{-4})T$$

$$\frac{dH^{o}_{m}}{dT} = 0.09 + (9.54\times10^{-5})T$$

Obviously, with the increase of temperature, the increasements of $C^0_{p,m}$ and S^0_m decrease, while that of H^0_m increases.

Gas-Phase Heats of Formation

Heat of formation is usually taken as the indicator of the "energy content" of a compound, it is very important to predict the heat of formation accurately. The gas-phase heat of formation ($\Delta_f H°_{gas}$) has been estimated using the above reaction. The experimental ($\Delta_f H°_{gas}{}^{exp}$) and predicted ($\Delta_f H°_{gas}{}^{pre}$) $\Delta_f H°_{gas}$ using the reaction of $NF_3 \cdot BF_3$ are shown in Table 1, we can see that the $\Delta_f H°_{gas}$ of the adduct is large and negative (-1266.09 kJ·mol^{-1}), which indicates the adduct is stable under atmospheric condition.

Table 1. Total energies (E_0) at the CBS-4M level and the gas-phase heats of formation

Compounds	E_0 (a.u.)	$\Delta_f H°_{gas}{}^{exp}$ (kJ·mol^{-1})	$\Delta_f H°_{gas}{}^{pre}$ (kJ·mol^{-1})
BF_3	-324.6964	-1135.60	
-NF_3	-354.2227	-132.09	
$NF_3 \cdot BF_3$	-678.9213		-1266.09

Condensed–Phase Heats of Formation

For a crystal, the lattice energy (E_{latt}) is important for predicting its structural and physicochemical properties such as polymorphism and growth morphology. E_{latt} can be calculated from the energy difference between the crystal ($E_{crystal}$) and the isolated molecules ($E_{molcule}$), i.e.,

$$E_{latt} = E_{crystal} - Z\ E_{molecule}$$

where Z is the number of molecules in unit cell and equals to 4 here. E_{latt} is therefore the energy required for vaporizing a crystal and represents the strength of cohesion or interaction between molecules in the solid state. A negative value of E_{latt} indicates an attractive intermolecular interaction in a crystal. The lattice energies of $NF_3 \cdot BF_3$ obtained at DFT GGA/RPBE level is -20.19 kJ·mol^{-1}.

E_{latt} was further used to evaluate the enthalpy of sublimation (ΔH_{sub}) using the following relationship [18]:

$$-\Delta H_{sub} = E_{latt} + E_{ZPE} + ZRT$$

A rough estimation of the ΔH_{sub} is obtained by neglecting the E_{ZPE} term, and the solid phase heat of formation ($\Delta_f H°_{solid}$) is then predicted from $\Delta_f H°_{gas}$:

$$\Delta_f H^\circ_{solid} = \Delta_f H^\circ_{gas} - \Delta H_{sub}$$

The calculated $\Delta_f H^\circ_{solid}$ of $NF_3 \cdot BF_3$ is -1276.37 kJ·mol^{-1}.

Crystal Structure

As is known, among the 230 space groups, over 80% organic crystals belong to 7 typical space groups based on the statistical data, which are $P2_1/c$, $P2_12_12_1$, P-1, Pbca, C2/c, Pna2_1 and $P2_1$ [19-22]. The chosen force field methods (Universal and Dreiding) are commnly used to do a global search in the above 7 space groups, and finally 7 most stable polymorphs are obtained, the polymorph with the lowest energy will be recommended as the reasonable crystal from (Table 2).

According to the principle the most possible polymorph usually possesses lower energy, it can be concluded from Table 2 that $NF_3 \cdot BF_3$ tends to crystalline in $P2_1/c$ from both Universal and Dreiding force field.

The density functional theory method DFT-GGA-RPBE was then performed to optimize the predicted packing $P2_1/c$, the corresponding cell parameters are a=6.93 Å, b=13.44 Å, c=5.79 Å, α=90.00º, β=116.60º, γ=90.00º, ρ=1.72 g·cm^{-3} (Figure 4).

Table 2a. Possible molecular packing for $NF_3 \cdot BF_3$ in 7 most possible space groups obtained from the universal force field

Space groups	***P*2$_1$/*c***	*P*2$_1$2$_1$2$_1$	*P*-1	*P*bca	*C*2/c	*P*na2$_1$	*P*2$_1$
Z	**4**	4	2	8	8	4	2
E/ kcal/mol/asym cell	**-7.92**	-7.73	-7.84	-7.85	-7.82	-7.86	-7.91
a/ Å	**4.49**	12.11	5.91	12.01	12.93	12.40	4.82
b/ Å	**14.22**	4.81	7.52	5.01	4.42	4.79	7.09
c/ Å	**6.59**	7.27	4.85	13.94	16.79	7.05	6.14
α/ º	**90.00**	90.00	86.84	90.00	90.00	90.00	90.00
β/ º	**82.57**	90.00	101.08	90.00	118.73	90.00	97.21
γ/ º	**90.00**	90.00	86.38	90.00	90.00	90.00	90.00
ρ/ g·cm^{-3}	**2.21**	2.18	2.18	2.20	2.19	2.20	2.21

Table 2b. Possible molecular packing for $NF_3 \cdot BF_3$ in 7 most possible space groups obtained from the Dreiding force field

Space groups	***P*2$_1$/*c***	*P*2$_1$2$_1$2$_1$	*P*-1	*P*bca	*C*2/c	*P*na2$_1$	*P*2$_1$
Z	**4**	4	2	8	8	4	2
E/ kcal/mol/asym cell	**-6.07**	-5.80	-5.98	-5.69	-5.95	-5.89	-5.93
a/ Å	**4.66**	6.24	4.76	8.823	17.71	12.70	6.35
b/ Å	**14.56**	8.82	11.35	15.61	4.79	4.94	7.30
c/ Å	**10.62**	8.36	6.82	6.75	13.06	7.29	4.97
α/ º	**90.00**	90.00	128.56	90.00	90.00	90.00	90.00
β/ º	**141.21**	90.00	73.23	90.00	124.40	90.00	98.01
γ/ º	**90.00**	90.00	126.98	90.00	90.00	90.00	90.00
ρ/ g·cm^{-3}	**2.04**	2.01	2.02	1.98	2.02	2.02	2.02

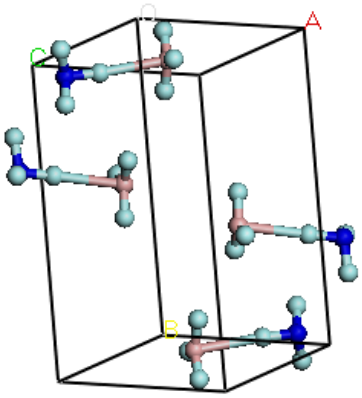

Figure 4. The optimized cell using DFT-GGA-RPBE method

Band Structure and Density of States

In principle, band gap (ΔE_g) between the highest occupied crystal orbital (HOCO) and the lowest unoccupied crystal orbital (LUCO) can be used as a criterion to predict the sensitivity of energetic materials with similar structure, and the smaller the ΔE_g, the easier the electron transits, and the larger the sensitivity will be. This principle has been illustrated by many experimental results and is useful both for the ionic crystals [23–27], and molecular crystals [28]. Figure 5 presents the band of the predicted most probable packing using the GGA-RPBE method, it can be seen that the ΔE_g of the title compound is large (6.06 eV) which denotes that the crystal form of the adduct is also stable.

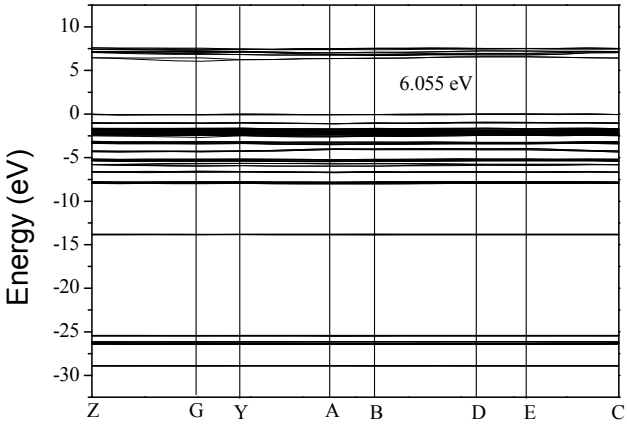

Figure 5. Banding structure of the title compound

Density of state is a presentation of the band structure of a crystal. A better understanding of the band structure is its PDOS, in which DOS is projected on atom-centered orbital, and PDOS can be used to investigate the constitution of energy bands. Figure 6 gives the DOS and PDOS of the predicted crystal structure using the GGA-RPBE method, and the origin of the energy is taken to be the Fermi level (the vertical dotted line). It is noted that the conduction band (LUCO) is mainly contributed from the *p* state of N atom and valence band (HOCO) from the *p* state of F atom.

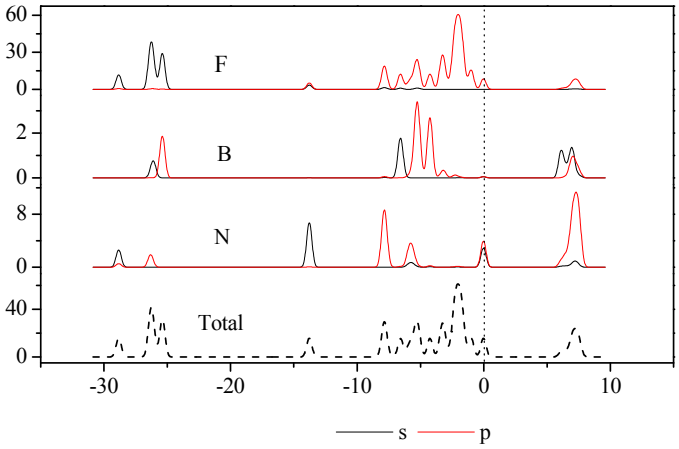

Figure 6. DOS and partial DOS of the adduct

CONCLUSIONS

The molecular and crystal structure of adduct $NF_3 \cdot BF_3$ has been investigated computationally using density functional theory. The adduct exists in complex form but not ionic. The heat of formation of the gas and condensed phase of the adduct are -1266.09 and -1276.37 $kJ \cdot mol^{-1}$, respectively. Its crystal tends to crystalline in $P2_1/c$ space group, the optimized cell parameters are a=6.93 Å, b=13.44 Å, c=5.79 Å, α=90.00º, β=116.60º, γ=90.00º, ρ=1.72 $g \cdot cm^{-3}$ under DFT-GGA-RPBE level. The calculated large band gap (6.06eV) proves the crystal is also stable, the conduction band (LUCO) is mainly contributed from the *p* state of N atom and valence band (HOCO) from the *p* state of F atom.

ACKNOWLEDGMENTS

This work was supported by Research and development Foundation (No. 2012FR057, 2013FR019, 2011FR005 and 2013FK026) of Zhejiang A & F University. National Natural Science Foundation of China (11304284, 51103136 and 51201153). The teaching project of Zhejiang A & F University (No.KG14342).

We are grateful for technical support and computer time at the Sugon server of the computer center of Nanjing University of Science & Technology.

REFERENCES

1. N.N. Greenwood, R. L. Martin, *Quart. Rev.,* **1954**, *8*, 1.
2. O. Ruff, J. Fischer, F. Luft, *Z. Anorg. Chem.,* **1928**, *172*, 417.
3. C.R. Bailey, J.B. Hale, J.W. Thompson, *J. Chem. Phys.,* **1937**, *5*, 274.
4. S. John, W. Gordy, *Phys. Rev.,* **1950**, *79*, 513.
5. V. Schomaker, Chia-Si Lu, *J. Am. Chem. Soc.,* **1950**, *72*, 1182.
6. H. Reichardt, A. Frenzel, K. Schober, *Microelectron. Eng.,* **2001**, *56*, 73.
7. T.A. Ford, D. Steele, *J. Phy. Chem.,* **1996**, *100*, 19336.
8. M.J. Frisch, G.W. Trucks, J.A. Pople, Gaussian-98, Revision A.7, Gaussian, Inc., Pittsburgh PA, **2003**.
9. M.W. Chase, C.A. Davies, J.R. Downey, D.J. Frurip, R.A. McDonald, A.N. Syverud, JANAF Thermochemical Tables, 3rd ed. *J. Phys. Chem. Ref. Data*, **1985**, 14, Suppl. 1.
10. T.L. Hill, Introduction to Statistic Thermodynamics, Addison-Wesley, New York, **1960**.
11. Materials Studio, Version 4.4, Accelrys Software, San Diego, **2008**.
12. A.J.C. Wilson, *Acta Crystallogr Sect A: Found Crystallogr.,* **1988**, *44*, 715.
13. A.D. Mighell, V.L. Himes, J.R. Rodgers, *Acta Crystallogr Sect A: Found Crystallogr.,* **1983**, *39*, 737.
14. R. Srinivasan, *Acta Crystallogr. Sect A: Found Crystallogr.,* **1992**, *48*, 917.
15. W.H. Bau, D. Kassner, *Acta Crystallogr. Sect B: Struct. Sci.,* **1992**, *48*, 356.
16. M.D. Segall, P.J.D. Lindan, M.J. Probert, C.J. Pickard, P.J. Hasnip, S.J. Clark, M.C.J. Payne, *J. Phys-Condens. Mat.,* **2002**, *14*, 2717.
17. S. Grimme, *Journal of Computational Chemistry,* **2006**, *27*, 1787.
18. C. Giacovazzo, Fundamentals of Crystallography, Oxford University Press: New York, **1992**.
19. A.J.C. Wilson, Space groups rare for organic structures. I. Triclinic, *Acta Crystallogr. Sect A: Found Crystallogr.,* **1988**, *44*, 715.
20. A.D. Mighell, V.L. Himes, J.R. Rodgers*, Acta Crystallogr. Sect A: Found Crystallogr.,* **1983**, *39*, 737.
21. R. Srinivasan, *Acta Crystallogr. Sect A: Found Crystallogr.,* **1992**, *48*, 917.
22. W.H. Baur, D. Kassner, *Acta Crystallogr. Sect B: Struct. Sci.,* **1992**, *48*, 356.
23. G. Wang, C. Shi, X. Gong, *J. Hazard. Mater.,* **2009**, *169*, 813.
24. H. Xiao, Y. Li, Banding and electronic structures of metal azides, Science Press, Beijing, **1996** (in Chinese).
25. W. Zhu, J. Xiao, H. Xiao, *J. Phy. Chem. B,* **2006**, *110*, 9856.
26. W. Zhu, J. Xiao, H. Xiao, *Chem. Phy. Lett.,* **2006**, *422*, 117.
27. X. Xu, H. Xiao, J. Xiao, *J. Phy. Chem. B,* **2006**, *110*, 7203.
28. W. Zhu, J. Xiao, G. Ji, *J. Phy. Chem. B*, **2007**, *11*, 12715.